Remote Mapping of Gas Flares in the Niger Delta with MODIS imagery

Obinna C.D. Anejionu, Alan Blackburn and Duncan Whyatt

Lancaster University, Lancaster Environment Centre, United Kingdom;
o.d.anejionu@lancaster.ac.uk

Abstract. More than fifty years of oil and gas exploration in the Niger Delta region of Nigeria has greatly endangered the ecosystem. Gas flaring, a process used to dispose gases associated with crude oil has been indicted as a prominent agent of pollution in the region. Efforts to empirically assess the environmental impacts of flaring have been hindered due to limited access to official information on flare locations and volumes. Consequently, there is a need to develop alternative methods of acquiring such information, and remote sensing seems the most viable option. To date, there have only been a limited number of studies on detecting and mapping flares from space. Flare detection methods have been developed based on Defence Meteorological Satellite Program Operational Linescan System (DMSP-OLS) and ATSR imagery, which have been employed in global estimation of flaring volume, but these techniques have some limitations. In our own previous research, we developed a flare detection technique based on the infrared bands of Landsat imagery, which was successfully applied to map active gas flares in the Niger Delta, between 1984 and 2012 with higher spatial precision than DMSP-OLS and ATSR based methods. However, because of the limitations imposed by the relatively low temporal resolution of Landsat, unavailability of night-time data, cloud cover and scanline correction error affecting Landsat images from 2003, we decided to extend the flare detection technique by employing imagery with a higher temporal resolution and moderate spatial resolution. In this paper, we describe the development of a flare detection method based on night-time Moderate Resolution Imaging Spectroradiometer (MODIS) thermal imagery. This single channel method involves the fusion of results obtained from the thresholding and spatial filtering of the thermal imagery. The method was validated using a database of flare locations derived from interpretation of high resolution aerial photography to achieve a user accuracy of 97% and producer accuracy of 81%. The method has been applied to the Niger Delta region and has successfully detected 165 active onshore and offshore flares from 2004 to 2008. Results obtained were further used to develop a model for estimating volume of gas flared over the study period. This will subsequently be used for the evaluation and modelling of the impact of flaring on the ecosystem. Furthermore, in the future the method developed will play a key role in monitoring Nigeria's compliance to the 30% gas flaring reduction target by the end 2017, recently set at the Global Forum of the World Bank-led Global Gas Flaring Reduction initiative.

Keywords. Gas Flare, Thermal Infrared Remote Sensing, MODIS Flare Detection, Niger Delta, Oil pollution

1. Introduction

The ecosystem of the Niger Delta region of Nigeria has greatly been endangered by ongoing oil and gas exploration, which commenced in 1958. Among the various activities associated with oil and gas exploration that directly affects the environment such as oil spillage and fire, deforestation, dredging and associated waste, gas flaring has been indicted as a prominent agent of pollution in the region. Gas flaring (Figure 1) is one of the processes (alongside venting and reinjection) used to dispose natural gases associated with crude oil. This process has commonly been adopted by all the oil companies operating in the region due to its cost effectiveness compared to the logical alternative of conversion of the gas to commercial natural gas. Efforts to empirically assess the environmental impacts of flaring have been hampered due to limited access to official information on flare locations and volumes. Thus, previous studies conducted by researchers have mostly been speculative or not comprehensive (focusing on a very small section of the region). Consequently, there is a need to develop alternative methods of acquiring such information, and remote sensing seems the most viable option. To date, there have only been a limited number studies on detecting and mapping flares from space. Flare detection techniques have been developed based on Defence Meteorological Satellite Program Operational Linescan System (DMSP-OLS) and Along Track Scanning Radiometer (ATSR) imagery which have been employed in global estimation of flaring volume, but these techniques have some limitations such as visual identification, subjective, time consuming, and difficulty in identifying flares amidst urban lights.

Figure 1. Shell gas flare at Kolo Creek, surrounded by agricultural fields [1].

In our previous research [2], we discussed the development of Landsat Flare Detection Method (LFDM), a gas flare detection method based on the infrared bands of Landsat imagery. The method was successfully applied to map active gas flares in the Niger Delta region of Nigeria, with higher spatial precision than DMSP-OLS and ATSR based methods; using available cloud-free images acquired from 1984 to 2012 to detect 212 flares (172 onshore and 40 offshore). The method, a multiband threshold technique that harnessed the flare detection potentials of near infrared, shortwave infrared and the thermal infrared bands of Landsat was considered novel especially in the high level of detail of detection obtained, which surpassed earlier methods based on low resolution imagery. The availability of a long archive of Landsat imagery also enabled us to look as far back as 1984 into the flaring history of the region. Despite its success in flare detection, the low frequency of available cloud-free images over the region, unavailability of night-time Landsat data, coupled with the SLC error, which affected most of the images from 2003; limited the employment of Landsat-based method in the development of a spectral technique for the estimation of volume of gas flared in the region. Therefore we decided to explore the potentials of Moderate Resolution Imaging Spectroradiometer (MODIS) imagery in gas flare detection and estimation of flaring volume. In a report in 2010, [3] demonstrated the potentials of MODIS imagery in this regard. We hope to achieve increased frequency of cloud free data over the region through the employment of images from Terra and Aqua platforms that would be suitable for a reasonable estimate of flaring volume. In this study, we set out to achieve the following objectives:

i. explore the gas flare detection potential of the MODIS imagery,
ii. develop a MODIS-based remote sensing technique for accurate detection of active gas flares,
iii. apply the technique in the survey, monitoring, and mapping of active flares in the region,
iv. develop a technique for the estimation of volume of gas flared from MODIS spectral radiance.

We thus, described in this paper, the development of MODIS Flare Detection Technique (MFDT), a flare detection method based on night-time MODIS thermal imagery. This single channel method involves the fusion of results obtained from the thresholding and spatial filtering of the MODIS thermal imagery (Band 22). The method was validated using a database of flare locations derived from high resolution aerial images. The method has been applied to the Niger Delta region and has successfully detected 165 active onshore and offshore flares from 2004 to 2006. The research was extended based on the flare detection results obtained, to develop a technique to estimate volume of gas flared from the spectral radiance of the thermal band. The flare volume estimation technique was subsequently applied to estimate flaring volume from 2004 to 2008, and result obtained closely correlating with available official records of annual flaring volumes in the region. Further work is ongoing to estimate the volume of gas flared over the period covered by the MODIS archive (2000 to present). This will be used in the evaluation and modelling of the impact of gas flaring on the Niger Delta ecosystem. Furthermore, the method is expected to play a key role in future monitoring of gas flaring across the region, and Nigeria’s compliance to the 30% gas flaring reduction target by the end 2017, recently set at the Global Forum of the World Bank-led Global Gas Flaring Reduction initiative.

1.1. Detection of gas flares using satellite imagery

Although gas flares are common features in oil and gas producing countries, only a small number of studies have attempted to detect them remotely. The suggestion that flares were detectable through satellite images was first made in 1978 by [4], having observed that they were visible in night-time Defence Meteorological Satellite Program (DMSP) and Landsat Multi-spectral Scanner System (MSS) images. By 1981, [5], discovered, while carrying out a research to determine blackbody temperatures of sub-pixel fires that flares were detectable from night-time NOAA-6 imagery. Twelve high temperature industrial sources in Detroit (steel mills), and six gas flares in the Persian Gulf oil fields were identified in the process using the 3.8µm and 11 µm sensors on board the NOAA-6 satellite. [6] visually inspected AVHRR images in order to identify gas flares from North Sea oil rigs. The DMSP Operational Linescan System (OLS) imagery was used by [7] to identify flares visually, using the circularity and bright centres of lights from flares to aid detection, and was the first to attempt flare detection on a global scale over a long period of time (1994-2008 inclusive). Although the DMSP method has high temporal resolution (12 hours revisit period), the relatively low spatial resolution (560m – 2.7km) of the imagery greatly limits its ability to accurately detect flares, particularly amidst urban lightings as noted by Elvidge *et al*. (2009a). Furthermore, the visual identification technique employed is subjective and time consuming.

Recently [8] applied an active flame detection algorithm (ALGO3) to night-time Along Track Scanning Radiometer (ATSR) shortwave infrared imagery to globally detect flares from 1991- 2009. The method is a single fixed threshold algorithm that mostly employs temporal persistence of hotspot pixels as an indicator of flaring activity, with the presence of industrial installations (identified from high resolution images available on Google Earth) used to validate the results. However, the low spatial resolution (1000m) of ATSR could reduce the spatial precision with which flares are detected. Furthermore, the method of validation may be inconsistent as not all industrial sites in oil producing regions contain flares. Nevertheless, ALGO3 is more objective than the DMSP and AVHRR methods, as it adopts a fixed threshold method to discriminate hotspots based on the spectral characteristics of ATSR imagery in the automatic detection of flares, thus overcoming the limitations of manual identification. The method has subsequently been revised through the integration of night-time ATSR and SAR products to detect flares in the North Sea [9].

Whilst the DMSP and ATSR methods of flare detection are quite useful for global studies of flaring, they may be of limited utility in studies across regional areas such as the Niger Delta, with more onshore than offshore flares (close to communities), and differing ecosystems and environmental conditions (mangrove to rain forest zones); where detailed survey and monitoring of flares is needed for accurate assessment of the environmental and health impacts of flares from local to regional scales. Furthermore, the temporal coverage (1991 to 2009) of the outputs from the analysis of DMSP and ATSR data [8], [10], limits the ability to comprehensively study the impact of flares in regions where gas flaring has been practiced over longer time periods. Hence, we exploited in our previous study the higher spatial resolution of Landsat imagery and its extended time-series for the detection of flares and assessment of the long term spatiotemporal variations in flaring. It is expected that due to the relative short period of coverage of MODIS compared to Landsat, results from both satellites could be combined to have a more robust and accurate gas flaring history and flaring volumes in the Niger Delta and future monitoring. The MODIS Flare Detection Technique (MFDT), developed in this research has been designed to provide an accurate and objective means of detecting onshore and offshore flares, using a transferrable and repeatable method that is simple, cheap, quick and efficient, and facilitates the derivation of flaring volumes from sensor signals.

1.2. Satellite imagery and fire detection

Satellite systems have long been deployed to detect and monitor fires and their effects, due to their timely and repetitive observations, multispectral viewing capabilities, information retrieval from hazardous locations and synoptic detection capabilities. Fire detection is based on the ability of sensors to identify signals produced by fire from space. The two main types of signal employed for this purpose are the direct (flames and heat) and the indirect (smoke and burned surfaces). The direct signals are most commonly employed in fire detection [11], [12], [13], while the indirect are employed for post fire assessment and management [14], [15]. Most satellite-based fire detection studies have focused on forest/biomass fires, as their impacts draw considerable attention from the research community and investigations are facilitated by the availability of well-validated fire-hotspot algorithms [16], [17]; [18], [19], [5], [20]. Fire detection from space is based on Planck's function (the temperature of a blackbody determines the characteristics of spectral radiation it emits).

$$\lambda_{\max} = \frac{C_w}{T} \tag{1}$$

Where:

$\lambda_{\max}$ = Wavelength where highest emitted radiance occurs

T = object temperature in K, and

C_w = Wien's constant ($\approx$2898μmK).

Radiation emitted at typical surface fire temperatures mostly lies in the infrared region of the electromagnetic spectrum. Thus, images from sensors such as Advanced Very High Resolution Radiometer (AVHRR), Moderate Resolution Imaging Spectroradiometer (MODIS), and Geostationary Operational Environmental Satellite (GOES), which have infrared bands, have mostly been used for forest fire detection [21], [12] [22], [18]. These systems also have relatively high temporal resolution, enabling near-continuous monitoring of active fire fronts, which is very important given the ephemeral nature of biomass fires.

The AVHRR was used to produce the first global fire product and near-real-time global fire data set. Fire detection capability of AVHRR was first applied on fixed targets of known location (gas flares in the Persian Gulf and high temperature industrial sources in Detroit) by [5] using NOAA-6 nighttime imagery. Daytime NOAA-6 data was similarly used to detect gas flares associated with oil fields in the North Sea [6]. The level of success achieved in the detection of fixed fire sources led to the use of AVHRR in biomass fire detection. Application of Dozier's methodology on AVHRR has also been used to study fire at sub-pixel level, to simultaneously determine temperature of fire and the proportion burning [23].

Further developments in remote sensing leading to the advent of MODIS sensor, greatly revolutionised the capability of fire detection from satellite images. With the availability of 36 spectral bands and special channels dedicated to fire monitoring, MODIS has improved the results of fire detection based on existing algorithms developed for AVHRR [23], [24].

Four major classes of algorithms (single channel threshold, multi-channel threshold, contextual, and sub-pixel fire detection algorithms), initially developed based on the dominating effects of hot fires in AVHRR Channel 3 signals, have mainly been used to detect fires from satellite images [18], [19].

2. Methods

2.1. Data and preprocessing

The main data used in this research include MODIS imagery, high resolution aerial photographs from Google Earth, and a political map of Nigeria delineating state boundaries, obtained from the Department of Geoinformatics and Surveying, University of Nigeria Nsukka. Cloud free day and night-time MODIS data from Terra and Aqua platforms covering the months of January and December from 2004 to 2008, which were acquired from the NASA's Earth Observing System Data and Information System (EOSDIS) (http://earthdata.nasa.gov/). Data from the months of January and December were chosen as they are less impacted by clouds, which is a limiting factor in remote sensing study of the Niger Delta. The chosen months fall within the Harmattan weather period, with drier and less humid conditions (thus, less cloudy), and it was assumed that the two months would be sufficiently reflective of annual trends in flaring activities in the region.

The MODIS raw DN values were processed to spectral radiances and reflectance (for band7) and georefrenced to WGS 1984 coordinate system, after which they were clipped to the study area. MODIS bands known to be sensitive to fire and hot temperature events (thermal bands 21 and 22, 31, and shortwave band 7) were examined. Band 21 and 22 were found to be sensitive to gas flares, as a good number of flares were visually identifiable on them (Figure 2). The two bands have almost similar response to gas flares, however, band 21imagery is known to be noisier, and with higher quantization error compared to band 22 [25]. Day-time reflectance and radiance of Band 7 was found to have some flare detection potential, however it was found be highly sensitive to other reflective materials including clouds, built-environment and sands in and around rivers. The night-time data of band 7 was not able to detect any feature including gas flares. Therefore any usefulness of band 7 day time data in flare detection could not be matched with the night-time equivalent, and was thus discarded as a resource for the research. There was no identifiable significant flare detection potential of day-time and night-time thermal band 31. Day-time band 21 and band 22 were found to be sensitive to other hot and reflective surfaces such as urban areas, bare lands and sands due to irradiation from the sun. Therefore, due to this solar irradiation impacts on day-time data, especially contributions from built environment, and the inherent noisy nature of band 21, a decision was made to use only night-time data from MODIS band 22 for improved accuracy.

Monthly composites of all available cloud free data within each study month was subsequently computed for use in the flare detection.

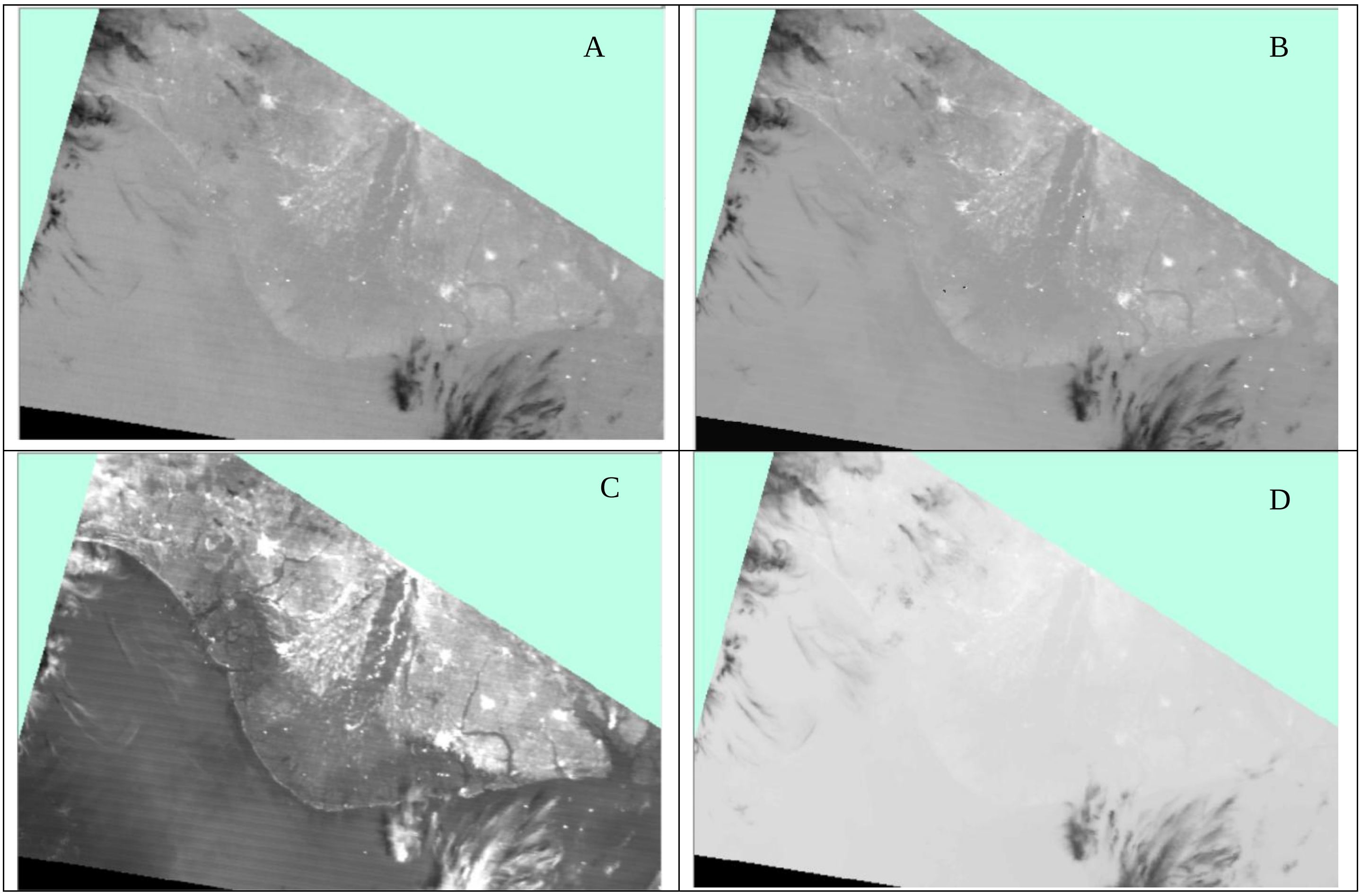

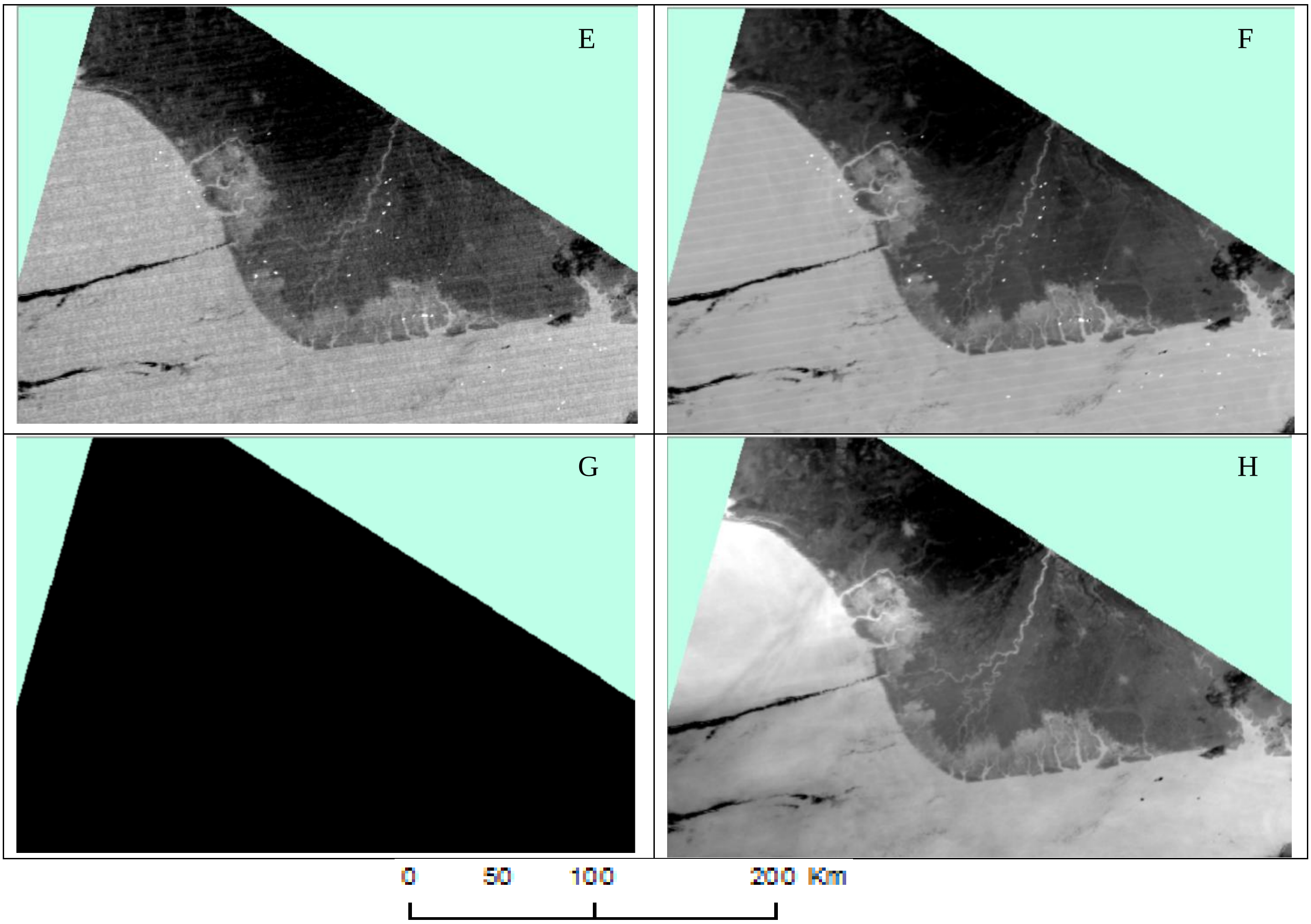

Figure 2. Illustration of flare detection potentials of various MODIS bands using data acquired on 01/12/2004 (Day-time) and 02/12/2004 (Night-time) with the Terra platform. (A) Day-time band 21 image, (B) Day-time band 22, (C) Day-time band 7, (D) Day-time band 31, (E), Night-time band 21, (F), Night-time band 22, (G) Night-time band 7, (H) Night-time band 31

2.2. Development of MODIS flare detection technique

Having observed that gas flares were detectable with MODIS thermal band 22, we tried to develop a technique that would accurately and automatically discriminate flares from other hot or highly reflective features. A single band-based algorithm that would utilise the spectral and spatial properties of gas flares was chosen. Gas flares are smaller in size than biomass fires and occur at flare pits permanently fixed to a particular location and are mostly continuously active [26], [27]. This continuous burning of gas is expected to generate a considerable amount of thermal signal that would distinguish it from background features. However due to the varying environmental conditions in the Niger Delta ranging from offshore, to mangrove swamp and to rainforest areas, which would result in lower gas flare thermal radiation in colder areas and higher flare radiation in warmer areas, we decided to use a fusion of traditional single band threshold algorithm (spectral), and contextual algorithm (spatial) that would be able to identify gas flares based on the difference between radiations from flare pixels and surrounding pixels [28]. Thus, using a spectral threshold to identify potential flares, and combining the result to the results obtained from a high pass spatial filtering and subsequent reclassification of same image (that would delineate the spatial extent of the high thermal response from flare pixels from surrounding background pixels). The spatial filtering is an adaptation of earlier methods used by [20], [28], in the identification of active fires and that of [3] carried out on the result of the difference between the signals received from band 22 (4μm) and band 31(11μm), while trying to identify flares from MODIS imagery. The combination of the spatial filtering and spectral thresholding was found to be quite effective especially for offshore flares where the sea surface was found to be quite reflective compared to land areas during the night.

In order to identify the optimal spectral radiance thresholds for the identification of flares from both the spectral and spatial components of the technique, various thresholds and combinations were tested. We decided that spectral threshold would be chosen on the basis that it would incorporate all potential flares in offshore and onshore areas, while the spatial threshold would isolate pixels where there is a significant spectral radiance difference with surrounding pixels. After careful interactive examination of the night-time data, average background pixel in the onshore areas (rain forest) was found to be about 0.53 Wm^{-2} sr^{-1} μm^{-1}, while that of the offshore areas and mangrove swamp areas were found to be 0.65 Wm^{-2} sr^{-1} μm^{-1} and 0.62 Wm^{-2} sr^{-1} μm^{-1} respectively. The following thresholds were thus tested for the spectral algorithm part of the technique: 0.56, 0.6, 0.645, and 0.66 (Wm^{-2} sr^{-1} μm^{-1}). The average background values in the filtered image was found to be 0.004 for offshore (sea) and onshore (land and mangrove areas), however rivers and creeks in the delta have slightly higher values that got up to 0.2 due to the difference between the narrow water bodies and surrounding pixels, and the average values were found to be 0.1. Therefore the following thresholds were tested for the spatial algorithm: 0.2, 0.3, 0.4, and 0.5 Wm^{-2} sr^{-1} μm^{-1}. The optimum thresholds were found to be 0.56 Wm^{-2} sr^{-1} μm^{-1} for the raw Band 22 image (spectral algorithm) and 0.3 Wm^{-2} sr^{-1} μm^{-1} for the filtered image (spatial algorithm) (see Section 2.3). Having established the optimal thresholds, the technique was subsequently implemented as shown in Figure 3.

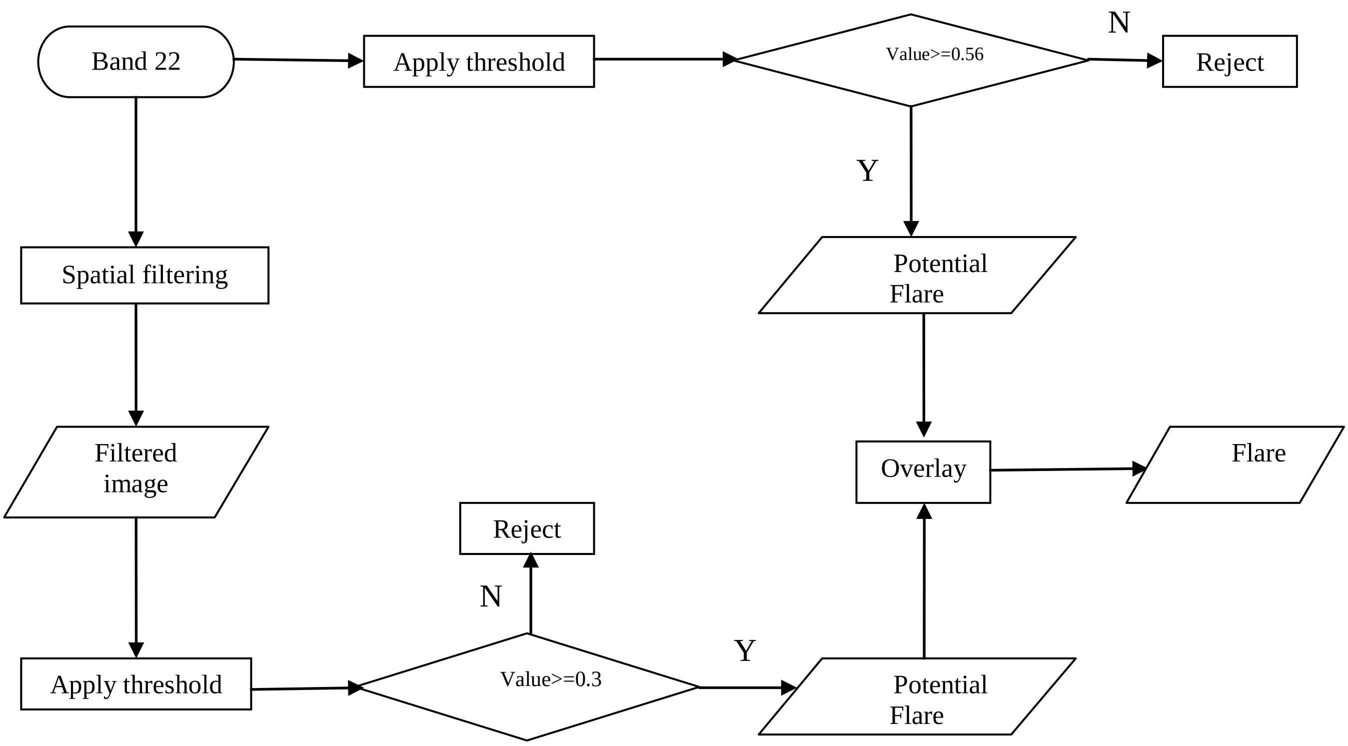

Figure 3. Flow chart illustrating the key stages of the MODIS Flare Detection Technique, based on the harnessing of the spectral and spatial properties of flares.

2.2.1. Validation of flare detection technique

High resolution images available on Google Earth covering the Niger Delta were visually analysed in order to construct a validation dataset of active flare locations. This approach was adopted because ground-based surveys of flare locations were not feasible at the time of research, due to logistical issues. A regular grid of 400m x 400m was superimposed on the high resolution images and this was used to systematically scan the entire study area to determine the locations of active flares. Visible fires from gas flares (Figure 4) were used in conjunction with clearly discernible physical structures such as buildings, pipelines, flare pits and flare stacks to confirm the locations of active flares. This method for collecting reference data on flare locations has been employed effectively by previous researchers [8], [29].

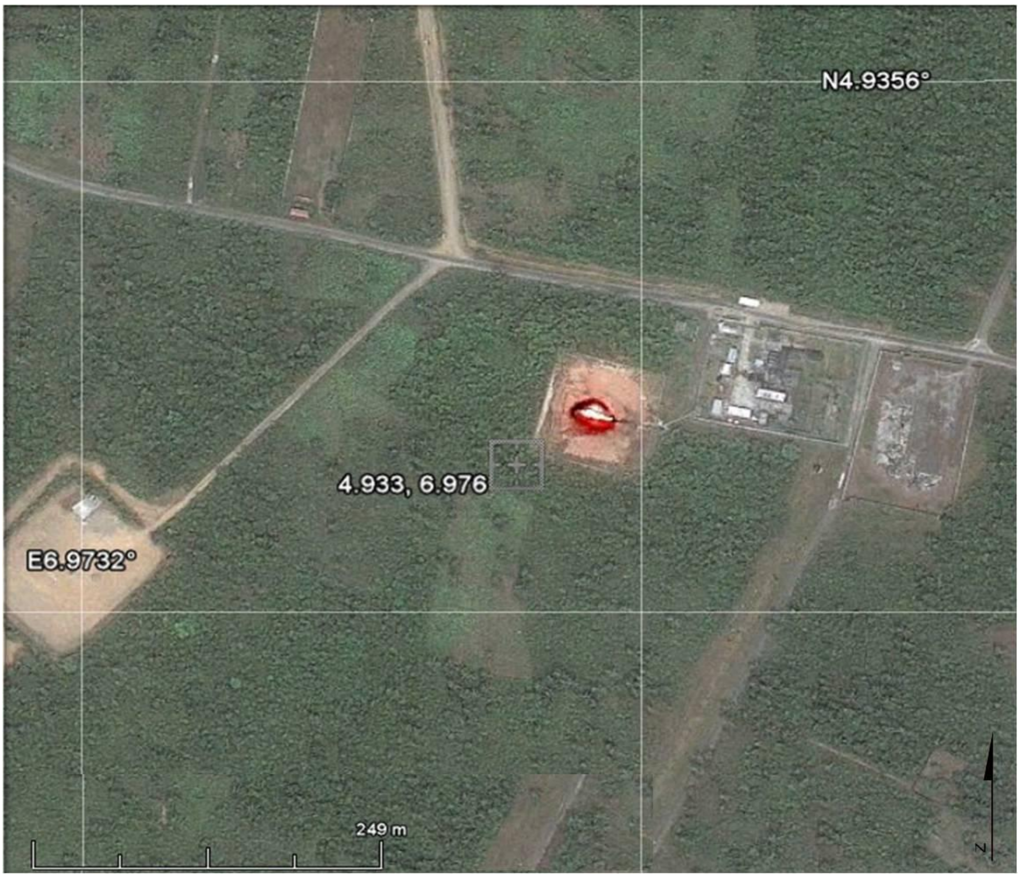

Figure 4. An active flare in the Agbada oilfield of Niger Delta captured on high resolution image on Google Earth

The high resolution imagery was therefore used to identify twenty gas flares found to be active in December 2006 and January 2007, which were used for validation (Table 1). Bearing in mind that gas flaring occurs at flow stations, the presence of an active flare is therefore a conclusive evidence of the presence of a flow station. As flaring is more or less a continuous process, it was assumed that locations where active flares have been identified from high resolution images, but where there were not subsequent high resolution images on Google Earth within the validation period to confirm further presence or absence of active flares, that such flares were still active. Therefore if the MFDT subsequently identified the locations as flare on dates different from the acquisition date of the high resolution image, it was assumed to be a correct identification. This approach was considered appropriate as processing of crude oil in flow stations is continuous as crude oil is gathered from various oil wells within the oilfield (disruptions in one or two oil wells would not necessarily affect operation at the flow station), and disposal of produced gas is necessarily due to safety reasons. Thus, an instant of high resolution image indicating active flare presence was assumed to be sufficient for at least within a forty one day period.

The active flare samples were grouped into different sets based on acquisition dates, and MODIS data matching these acquisition dates were used in conjunction with composites obtained by expanding on both sides of the most central sample date or the date with highest number of samples until a full month composite of available MODIS data was obtained. As the number of samples in each set was considered not large enough for a good accuracy assessment, two different groups of accuracies were compiled based on samples from actual dates of acquisition of high resolution images and the total samples identified within the validation period. These were matched with the single image and the different image composites for each study month. For example, three flares found to be active on the 7^{th} of December 2006, from high resolution image would be used to compute one set of user and producer accuracy from result obtained from MODIS data acquired on the 7^{th} of December 2006, and another set of accuracies would be computed based on all the twenty samples found to be active within the 41 days validation period. Subsequently, four validation samples (3 for 7^{th} and 1 for 4^{th}) would be used to compute one set of accuracies for a composite of images acquired from the 4^{th} to the 7^{th} of December 2006, and then another from the 20 samples.

Table 1. Validation samples obtained from high resolution images showing acquisition dates and summary of samples per acquisition date

Sample	**Date**	**January 2007**	
Flare 1	07/12/2006	**Sample**	**Number**
Flare 2	09/01/2007	09/01/2007	6
Flare 3	07/12/2006	06/01/2007	2
Flare 4	14/01/2007	03/01/2007	1
Flare 5	29/12/2006	14/01/2007	4
Flare 6	29/12/2006	**Total**	**13**
Flare 7	06/01/2007		
Flare 8	06/01/2007	**December 2006**	
Flare 9	14/01/2007	**Sample**	**Number**
Flare 10	14/01/2007	07/12/2006	3
Flare 11	03/01/2007	04/12/2006	1
Flare 12	07/12/2006	29/12/2006	3
Flare 13	29/12/2006	**Total**	**7**
Flare 14	09/01/2007		
Flare 15	14/01/2007		
Flare 16	09/01/2007		
Flare 17	04/12/2006		
Flare 18	09/01/2007		
Flare 19	09/01/2007		
Flare 20	09/01/2007		

To assess the accuracy of the technique, pixels identified as flares from the technique were compared to the validation samples, and where there is a match (intersection) between the locations of the samples and the pixels identified as flares by MFDT, a correct identification was recorded. In computing the user accuracy, known locations of flow stations in addition to active flares were used. The number of correct and incorrect identifications were noted and used to compute the relevant accuracies (user and producer accuracy). The technique aimed at obtaining a very high user accuracy (the percentage of the total flares identified by the MFDT that were correctly identified), while maintaining a reasonable producer accuracy (percentage of known flare locations that were correctly identified by the technique). This interest in higher user accuracy was considered appropriate as the focus was on maximising the proportion of correct identifications and higher user accuracy implies higher confidence in the use of the flare detection technique.

Based on the foregoing, the various thresholds (spectral and spatial) were tested on single and composite images acquired within the validation period. The mean of the accuracies obtained was computed and used in conjunction with total number of correct identifications to select the optimal threshold. The combination with the best balance of user accuracy, producer accuracy, and number of correct identifications was chosen as the optimal thresholds (Table 2). Therefore, a decision was made to use the thresholds of combination H with 97% user accuracy and 81% producer accuracy, as the optimum thresholds.

Table2. Summary statistics of average accuracies computed from the different threshold combinations based on single and composite images

All 20 Samples								Targeted Samples	
Name	**Spectral Threshold**	**Spatial Threshold**	**Total Detection**	**Samples Detected**	**Detections Confirmed**	**Producer Accuracy**	**User Accuracy**	**Samples Detected**	**Producer Accuracy**
A	0.660	0.4	56.5	13.9	54.4	69.7	98.3	5.4	73. 3
B	0.645	0.4	57.4	14.3	56.5	71.7	98.6	5.3	70.0
C	0.600	0.4	60.5	15.5	58.7	77.7	97.2	5.7	76.7
D	0.560	0.4	63.4	15.8	60.5	79.2	95.8	5.8	80.1
E	0.600	0.2	87.3	17.5	75.0	87.5	87.7	6.3	87.3
F	0.600	0.3	68.0	16.4	66.0	82.2	97.4	6.0	80.1
G	0.600	0.5	56.9	14.9	55.2	74.5	97.5	5.4	72.1
H	0.560	0.3	65.5	16.1	63.4	80.7	96.9	6.0	80.1
Summary of average derivations from monthly composites (January 2007 and December 2006)									
A	0.66	0.4	67.5	16.5	65	82.5	96.3	8	81.3
B	0.645	0.4	67.5	16.5	65.5	82.5	97.1	8	81.3
C	0.6	0.4	71.5	16.5	69	82.5	96.6	8	81.3
D	0.56	0.4	73	16.5	69.5	82.5	95.4	8	81.3
E	0.6	0.2	92	18.5	84	92.5	91.3	8.5	88.5
F	0.6	0.3	78.5	16.5	75	82.5	95.7	8	81.3
G	0.6	0.5	67	16.5	64	82.5	95.9	8	81.3
H	0.56	0.3	78	16.5	76	82.5	97.5	8	81.3

2.2.2. Flare detection with MFDT

Having determined the optimum thresholds for flare detection, the technique has so far been applied to monthly composites of MODIS data acquired in the months of January and December from 2004 to 2008. The number of times each flare was detected was recorded and flares that were detected only once out of the ten independent occasions were removed as false detections. This was in line with the assumption that flares are continuous and should be detected at least on two occasions within a four year period. However, false detections arising from biomass fires, or other ephemeral high reflectance features should not reoccur at the same location twice in a one month detection interval. Previous studies [8], [9], have utilised similar persistence approach in discriminating flares from false identifications or normalise the impact of background noise on flare detections [10]. The flares identified within this study period were used to obtain a flaring history model detailing the spatial and temporal variations in the distribution of active flares in the region. The Nigerian political map was used to allocate the detected flares to the different states in the region. As the map did not delineate the offshore boundaries of the states, offshore flares where objectively allocated to the nearest states using GIS tools in order to adequately represent the flaring activity of the states. Subsequently, the flares identified were further explored to determine the relationship between the spectral radiance and volume of gas flared.

2.3. Gas flare volume estimation with MODIS

Working from the assumption that quantity of gas flared at each location would determine the intensity of fire at the location, we tried to investigate the relationship between the volume of gas flared at each flare location to the spectral radiance emitted by flare and captured by the imagery. Monthly flaring volume records were obtained from the annual report of the Nigerian National petroleum Corporation (NNPC) [30]. We explored various options in this regard. The identity of twenty five flow stations linked to the flares detected were obtained and used to match the NNPC's flaring volume record. Three main approach were investigated before arriving at a satisfying relationship.

In the first approach, the centriods of the pixel/s identified as flares were calculated, and a buffer of 2500m radius (2 and half pixels) was used to extract statistical values based on the spectral radiance around the flares. The buffering radius was chosen in such a way as to incorporate the influence of the flares around surrounding pixels. It was thus expected that bigger flares would in general have greater influence on their surroundings than smaller flares. The various statistical values extracted (mean, sum, max, standard deviation) were used in conjunction with corresponding volume of gas flared to generate a regression analysis. Furthermore, different combinations (max x sum etc) and derivations (such as the difference of the sum and the background values) of the statistical parameters were also used in regression. Having obtained the various regression equations, they were tested using statistics derived from all the flares identified in December 2004 in order to validate them. Validation was carried out by using regression equations derived from the various parameters and combinations to apply to corresponding parameters/combinations based all identified flares for the month. The sum of all the estimated volume of gas flared was compared with the recorded total volume of gas flared for the month and differences noted as estimation errors. Equations with lowest estimation errors was chosen as optimal.

The result obtained from all the equations derived from the first approach were deemed not satisfactory as the difference between the estimated and recorded volume ranged from ± 0.13 billion cubic metres (BCM) to ± 0.96 BCM.

The second approach involved the use of polygons derived from only the pixels identified as flare pixels to extract the statistical values. This showed a slightly better accuracy of estimation compared to the first approach with estimation errors raging from ±0.04 BCM to ±0.3BCM. The equation generated from the sum was found to have the best estimation accuracy among all those tested in this approach.

Having realised that most big flares (with influence spanning across more than two pixels were undersampled by the second approach, we decided to apply a buffer with a radius of 1000m (1 pixel) around the pixels identified as flares. This was expected to incorporate surrounding pixels (hot pixels that were not identified as flares), where the influence of each flare would be felt, thus the sizes of the buffers directly varied with the sizes of the flares. In this way, the influences of large and small flares were expected to be effectively captured. The statistical parameters were extracted as usual and regression equations obtained (Figure 5) tested.

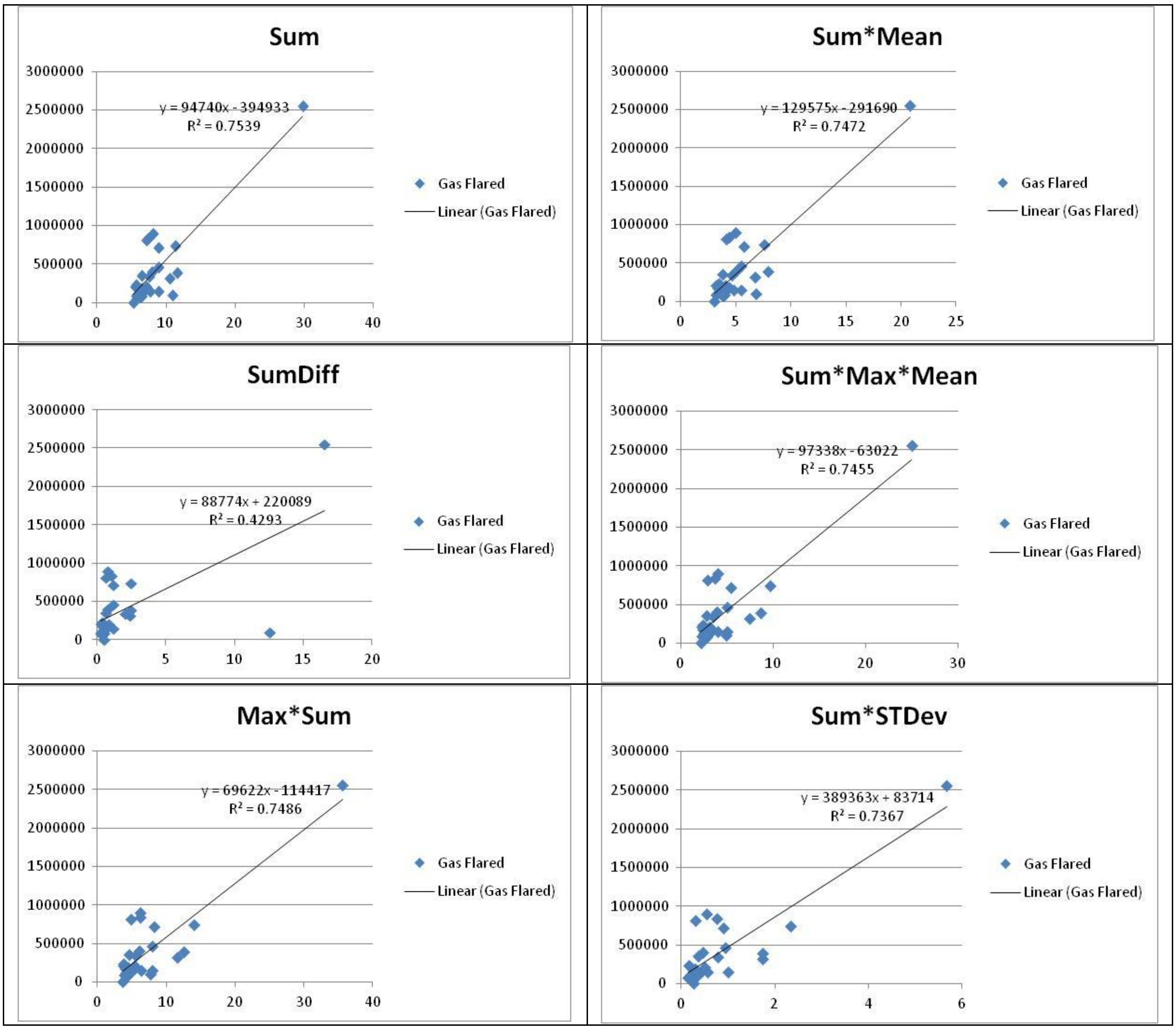

Figure 5. Scatterplots and equations obtained from the regression analysis of various statistical parameters and recorded volume of gas flared at sample flow stations in the Niger Delta.

Reduced estimation errors were obtained from this third approach as shown in Table 3. Regression equation derived from the product of Sum and Standard Deviation (Sum* StDev), and that from Sum were found to have the lowest estimation errors. The robustness was checked with other months and the equation from the sum was observed to be better in estimating flaring volumes across the years. The flare volume estimation equation developed is:

$$\textbf{\textit{Volume of gas flared}} = 94740 * Sum - 394933 \quad (2)$$

Where:
Sum = the sum of all spectral radiance within 1pixel buffer of detected flare pixels
$R^2 = 0.7539$

Table 3. Volume of gas estimations errors derived from various statistical parameters obtained from MODIS Band 22 spectral radiance

	Sum	**SumDiff**	**Sum*Max**	**Sum*Mean**	**Sum*max*mean**	**Sum*Stdv**
Estimated Total(Mscf)	67466529	31083479	75761168	79040286.9	87864230.1	66997668.3
Estimated Total(BCM)	1.9107	0.8803	2.14556	2.2384	2.4883	1.8974
Actual (Mscf)	67,079,747	67,079,747	67,079,747	67,079,747	67,079,747	67,079,747
Actual (BCM)	1.8996	1.8996	1.8996	1.8996	1.8996	1.8996
Error (Mscf)	-386,782	35,996,268	-8,681,421	-11,960,540	-20,784,483	82,079
Error(BCM)	**-0.011**	**1.02**	**-0.25**	**-0.34**	**-0.59**	**0.002**

*Mscf = Million Standard Cubic Feet

2.3.1. Volume of gas flared in Niger Delta (2000 – 2013)

The volume estimation model has so far been used to estimate the volume of gas flared from 2004 and 2008. Mean of the estimates obtained January and December of each year was used as the average annual flaring volumes. This was subsequently multiplied by 12 to obtain the total volume of gas flared in each year. Efforts are ongoing to estimate the volume of gas flared from 2000 to 2013 (covering the MODIS data archive range). Attempt would to be made to link the equation to spectral radiances derived from Landsat, so that earlier images in Landsat such as those from 1984 to 2000 could be used to estimate volume of gas flared in those periods. This is expected to result in a comprehensive understanding of the total volume of gas flared in this region, which would play a key role in the evaluation of the impact of gas flaring on the ecosystem, which would to be carried out at a later stage of this research.

3. Results

3.1. Mapping Flares in Niger Delta

The MODIS Flare Detection Technique developed in this research has so far detected 165 active flares in the Niger Delta from January 2004 to December 2008. Figure 6 shows the distribution and persistence of the flares across the various states of Niger Delta. One hundred and seven (107) onshore flares and fifty eight (58) offshore flares were detected by the MFDT. Out of theses detections, majority of the onshore flares were found to be located in Rivers state with 43 gas flares, while the majority of the offshore flares were located in Akwa Ibom State with 24 gas flares (Table 4).

Table 4. Distribution of flares across the Niger Delta States

State	All flares	Onshore flares	Offshore flares
Rivers	53	43	10
Delta	34	24	10
Bayelsa	26	19	7
Akwa Ibom	25	1	24
Edo	7	7	0
Ondo	10	3	7
Imo	9	9	0
Abia	1	1	0
Total	165	107	58

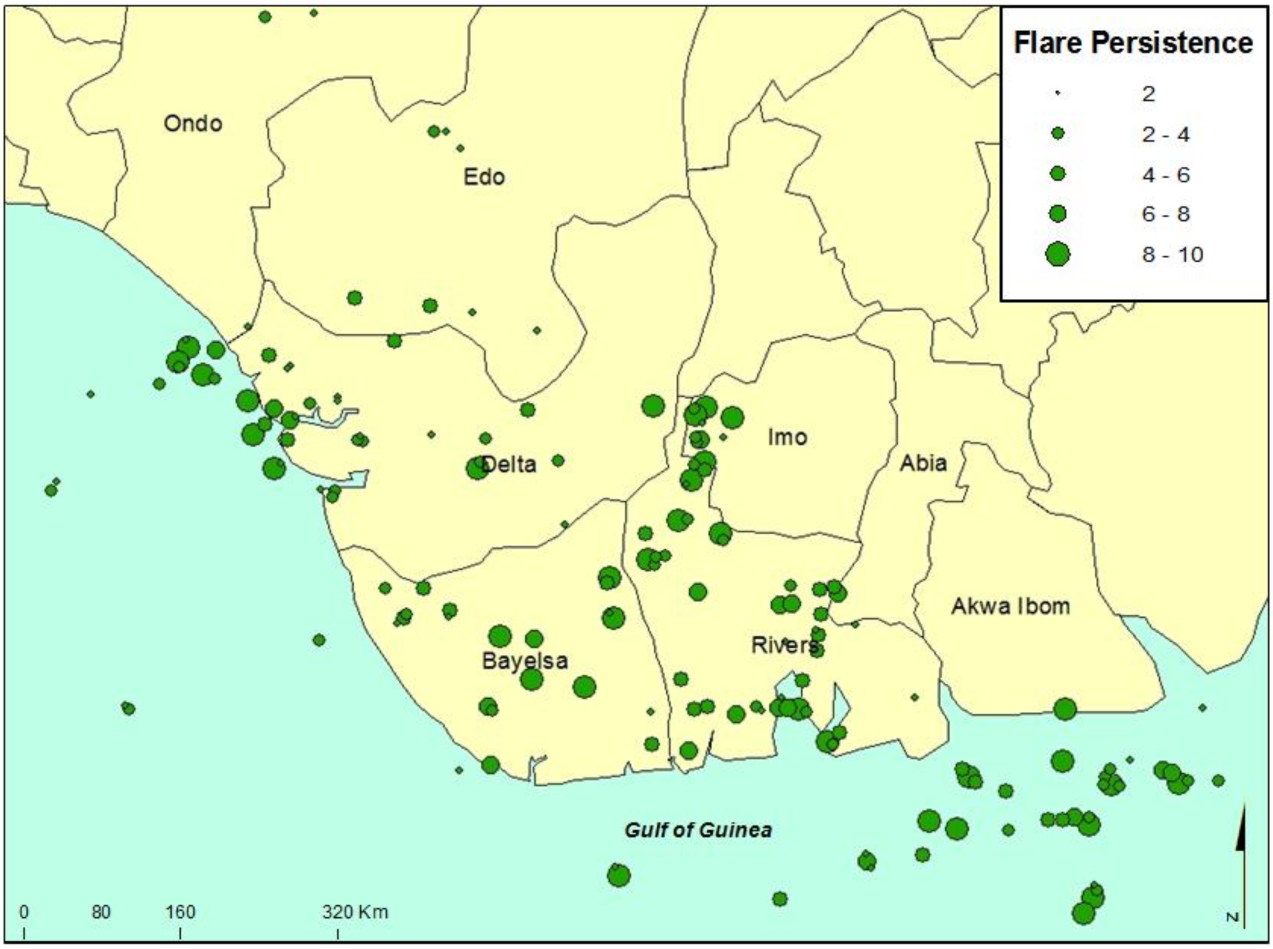

Figure 6. Map showing the spatial distribution of all flares identified in the Niger Delta with MODIS Flare Detection Technique from January 2004 to December 2008. The number of occasions each flare was detected is depicted with the size of the circle.

3.2. Estimating flaring volume with MODIS

The volume estimation model developed in this research showed that the highest volume of gas flared in the Niger Delta occurred in 2004 with 24.7BCM of gas flared in this year. The plot of all the annual volumes so estimated is shown in Figure 7. The plot shows a close correspondence with actual volume of gas flared that has been recorded. The average accuracy of estimation across all the years considered was found to be ±0.2BCM, which is a great improvement from those derived from DMSP (±2.11BCM) based on the model: BCM=0.0000266*Sum of lights index [31]. The total volume of gas flared in this study period was estimated to be 108.03billion cubic meters. This is quite an enormous amount of gas with associated high level of pollutants emitted. From the technique the volume of gas flared from each flow station could be readily obtained from MODIS imagery. This would be highly relevant in evaluating the impact of each flare on surrounding environment.

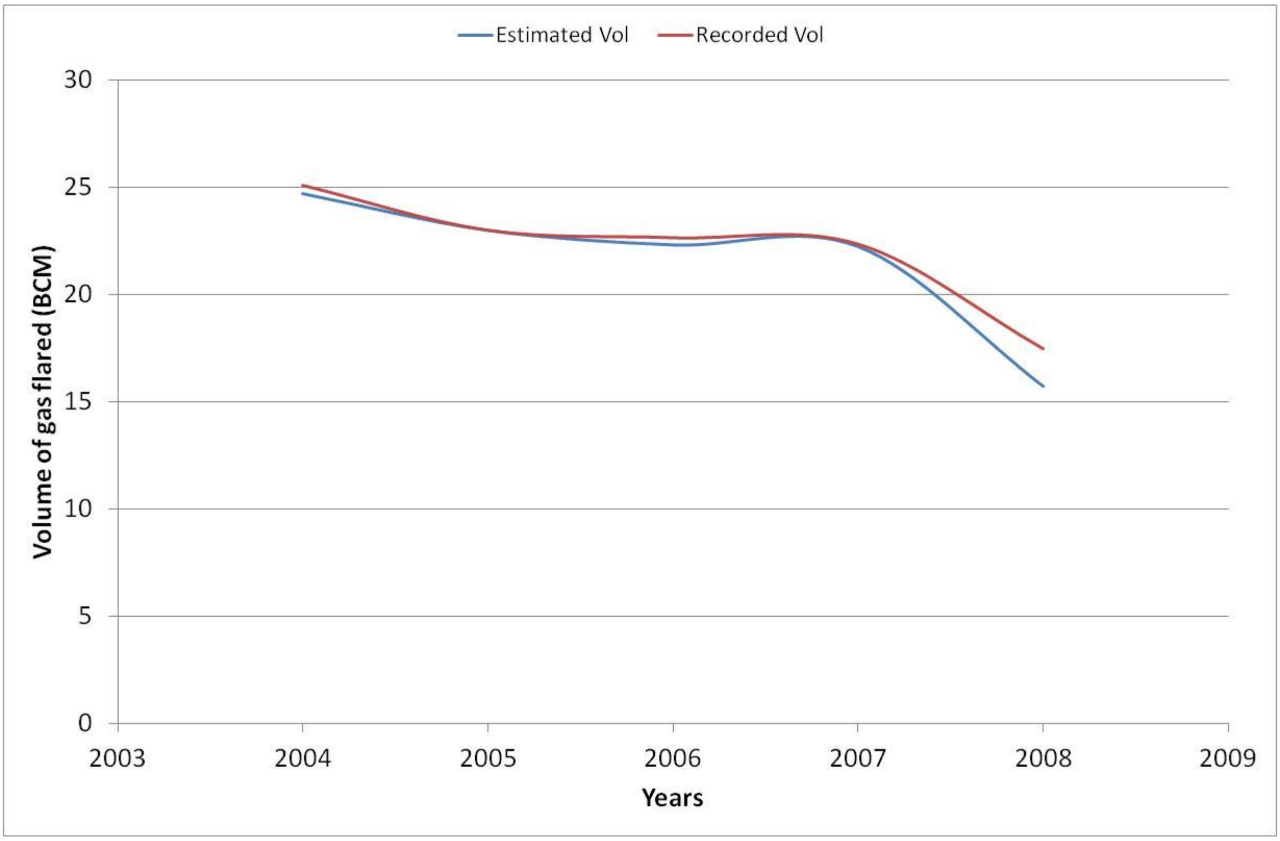

Figure 7. Plot showing the recorded and estimated volume of gas flared from 2004 to 2008. The close correspondence of the estimation is clearly depicted.

4. Conclusions

Gas flaring is a key agent of environmental pollution in the Niger Delta region of Nigeria. This research has greatly improved ongoing efforts to detect gas flares and estimate the volume of gas flared from flow stations from information available on satellite images. We described in this paper the development of a simple, automatic, objective, cost effective and accurate method of detecting gas flares and estimating flaring volume from MODIS imagery. The flare detection technique developed in this research is a single band based method, combining spectral threshold with spatial threshold (contextual) to retrieve gas flaring information from night-time MODIS thermal band 22 (4μm). The technique was duly validated with a reference dataset of gas flares obtained from high resolution aerial photographs, with a user accuracy of 97% and producer accuracy of 81%. The technique overcame most of the limitations of earlier studies (such as difficulty in detecting flares amidst urban lighting, visual identification of flares and the use of industrial complex for flare validation), and those of conventional surveying methods (such as being tedious, time consuming, involving high cost of execution). A total of 165 (107 onshore and 58 offshore) flares has so far been detected from the January 2004 to December 2008. It is worthy to mention that due to the resolution of the MODIS data (1000m), there is a possibility that not all the active flares in the Niger Delta within the study period were detected by our technique, especially smaller flares with lower intensity.

The flaring estimation model developed in this research was used to estimate annual volumes of gas flared from 2004 to 2008. It was found that about 108.03billion cubic metres of gas have been flared in the region within this study test period.

This research is very significant as it has improved the flaring estimations with an increased volume estimation accuracy of 0.2BCM compared to ±2.11BCM from earlier estimation accuracies obtained from DMSP. The flare detection technique is quite simple, objective and accurate and could effectively be employed for future monitoring of flaring activities in the region. There is also a great possibility of extending this technique into a global flare detection and volume estimation technique as the technique is quite transferable. This would be expected to play a key role in the ongoing Global Gas Flaring Reduction (GGFR) global satellite gas flaring detection and volume estimation initiative of the Word Bank. Furthermore, the result obtained would play a major role in the comprehensive evaluation of the impact of gas flaring on the Niger Delta ecosystem. The results are also expected to form an invaluable reference point for future gas flare related environmental and socioeconomic research in the Niger Delta region.

Further work leading from this research will focus on the development of an improved technique that would incorporate day-time MODIS data, which were not used in the present research due to the influence of solar irradiation on high reflectance features. The technique will subsequently be applied to an extended time series of MODIS from 2000 to 2013. This would lead to the estimation of total emissions from the identified flares and modeling of the impacts on the environment. An attempt would also be made to extend this work to other known gas flaring locations around the word.

Acknowledgements

We wish to acknowledge the Surveyors Council of Nigeria (SURCON), who partly supported the initial stages of this project with a research grant, the Department of Geoinformatics and Surveying, University of Nigeria Enugu Campus, for the provision of the political map used in this research and the Petroleum Technology Development Fund (PTDF Nigeria) who sustained the later stages of this research via a Scholarship. Thanks also to Lancaster University for the award of William Ritchie Travel Grant, Lancaster Environment Centre and Faculty of Science and Technology Lancaster University for the awards of travel grants for the conference.

References

[1] Friends of the earth. 2004. *Shell oil and gas flaring in Nigeria*. http://www.foe.co.uk/resource/images/shell_nigeria_2006/slides/EG_Gas%20flare%20Kolo%20Creek%20shot%201.html (accessed on 5th October, 2009).

[2] Anejionu, C.D.O**.,** Blackburn, G.A., and Whyatt, J.D. 2012. *Improving remote survey of gas flaring in the Niger Delta region of Nigeria with Landsat imagery*. Presentation at the 2012 GIS Research UK (GISRUK) Conference at Lancaster University, United Kingdom, and published in the Conference Proceedings.

[3] Elvidge, C.D., Baugh, K.E., Ziskin, D., Anderson, S., Ghosh, T., 2011. *Estimation of gas flaring volumes using NASA MODIS Fire detection products*. Report presented to NASA.

[4] Croft, T.A. 1978. *Nighttime images of the earth from space*. Scientific American, 239, 68-79.

[5] Matson, M. and Dozier, J. 1981. *Identification of subresolution high temperature sources using a thermal IR sensor*. Photogrammetric Engineering and Remote Sensing, 47:1311.

[6] Muirhead, K., and Cracknell, A.P. 1984. *Identification of gas flares in the North Sea using satellite data*. International Journal of Remote Sensing, 5, (1), 199 - 212.

[7] Elvidge, C.D., Baugh, K.E., Tuttle, B.T., Howard, A.T., Pack, D.W., Milesi, C., and Erwin, E.H. 2007. *A twelve year record of national and global gas flaring volumes estimated using satellite data. Final report to the World Bank*. http://siteresources.worldbank.org/INTGGFR/Resources/DMSP_flares_ 20070530_b-sm.pdf (accessed on 11th October, 2009).

[8] Casadio, S., Arino, O., Serpe, D., 2012, *Gas flaring monitoring from space using the ATSR instrument series*. Remote Sensing of Environment, 116, 239–249.

[9] Casadio, S., Arino, O. and Minchella, A. 2012. *Use of ATSR and SAR measurements for the monitoring and characterisation of night-time gas flaring from off-shore platforms: The North Sea test case*. Remote Sensing of Environment 123 (2012) 175–186.

[10] Elvidge, C.D., Ziskin, D., Baugh, K.E., Tuttle, B.T., Ghosh, T., Pack, D.W., Erwin, E.H. and Zhizhin, M. 2009a. *A fifteen year record of global natural gas flaring derived from satellite data*. Energies, 2, 595-622.

[11] Movaghati, S., Samadzadegan, F., and Azizi, A. 2009. *An Agent-Based Approach for Regional Forest Fire Detection using MODIS Data*. Journal of Applied Sciences 9 (20), 3672 - 3681.

[12] Justice, C., Giglio, L., Boschetti, L., Roy, D., Csiszar, I., Morisette, J., and Kaufman, Y. 2006. *Algorithm Technical Background Document: MODIS Fire Products*. http://modis.gsfc.nasa.gov/data/atbd/atbd_mod14.pdf. (accessed on 10th March, 2011).

[13] Weaver, J. F., Lindsey, D. T., Bikos, D. E., Schmidt, C. C., and Prins, E. 2004. *Fire detection using GOES-11 rapid scan imagery*. Weather and Forecasting, 19, 496-510.

[14] Lanorte, A., Danese, M., Lasaponara, R., and Murgante, B. 2011. *Multiscale mapping of burn area and severity using multisensor satellite data and spatial autocorrelation analysis*. International Journal of Applied Earth Observation and Geoinformation xxx (2011) xxx–xxx

[15] Sedano, F., Kempeneers, P., San Miguel, J., Strobl, P., Vogt, P., 2013. *Towards a pan European burnt scar mapping methodology based on single date medium resolution optical remote sensing data*. International Journal of Applied Earth Observation and Geoinformation, 20, 52-59.

[16] Dozier, J. 1981. A method for satellite identification of surface temperature fields of subpixel resolution, Remote Sensing of Environment, 11:221-229.

[17] Giglio, L., Descloitres, J., Justice, C.O., Kaufman, Y.J. 2003. *An enhanced contextual fire detection algorithm for MODIS*. Remote Sensing of Environment 8, 273–282.

[18] Li, Z., Kaufman, Y.J., Ichoku, C., Fraser, R., Trishchenko, A., Giglio, L., Jin, J., and Yu, X. 2000. *A review of AVHRR-based active fire detection algorithms: principles, limitations, and recommendations*. http://www.fao.org/gtos/gofc-gold/docs/fire_ov.pdf. (accessed on 4th February, 2011).

[19] Martín. M. P., Flasse, S., Downey, I., and Ceccato, P. 1999. *Fire detection and fire growth monitoring using satellite data*. http://publiclibrary.rfs.nsw.gov.au/CommonDocuments/7300FiredetectionMicrosoft%20Word%20-%20review.pdf. (*accessed on 10th March, 2011*).

[20] Prins, E.M., and Menzel, W.P. 1992. *Geostationary satellite detection of biomass burning in South America*. International Journal of Remote Sensing, 13 (15), 2783-2799.

[21] Ichoku, C., Kaufman, Y. J., Giglio, L., Li, Z. Fraser, R. H., Jin, J.Z., and Park, W. M. 2003. *Comparative analysis of daytime fire detection algorithms using AVHRR data for the 1995 fire season in Canada: perspective for MODIS*. International Journal of Remote Sensing, 24 (8), 1669–1690.

[22] Kaufman, Y.J., Justice, C., Flynn, L., Kendall, J., Prins, E., Ward, D.E., Menzel, P., and Setzer, A. 1998. *Monitoring Global Fires from EOS-MODIS*. Journal of Geophysical Research, 103, 32215-32338.

[23] Casanova, J.L., Calle, A., Romo, A., and Sanz, J. 2005. *Forest fire detection and monitoring by means of an integrated MODIS-MSG system*. Remote Sensing Laboratory of University of Valladolid. http://www.iki.rssi.ru/earth/articles/sec9_12.pdf (accessed on 12th February, 2011)

[24] Justice, C.O., Giglio, L., Korontzi, S., Owens, J., Morisette, J.T., Roya, D., Descloitres, J., Alleaume, S., Petitcoline, F. , Kaufman, Y. 2002. *The MODIS fire products*. Remote Sensing of Environment 83 (2002) 244 – 262.

[25] Giglio, B., Descloitres, J.,Justice, C.O., and Kaufman, Y.J. 2003. *An Enhanced Contextual Fire Detection Algorithm for MODIS*. Remote Sensing of Environment 87 (2003) 273 – 282.

[26] Friends of the earth. (2005). *Communities sue Shell to stop Nigerian gas flaring*. Archived press release. http://www.foe.co.uk/resource/press_releases/communities_sue_shell_to_s_20062005.html (accessed on 5th October, 2009).

[27] Shell Petroleum Development Company of Nigeria (SPDC), 2011. Shell in Nigeria: Gas flaring. http://www-static.shell.com/static/nga/downloads/pdfs/briefing_notes/gas_flaring.pdf. (*accessed on 8th December, 2011).*

[28] Flasse, S.P., Ceccato, P.S. 1996. *A contextual algorithm for AVHRR fire detection*. International Journal of Remote Sensing 17, 419 – 424.

[29] Elvidge, C.D., Baugh, K.E., Tuttle, B.T., Ziskin, D., Ghosh, T., Zhizhin, M., and Pack, D.W. (2009b). *Improving satellite data estimation of gas flaring volumes*. Year two final report to the GGFR.http://www.ngdc.noaa.gov/dmsp/interest/flare_docs/NGDC_flaring_report_20090817.pdf. (*accessed on 1st February 2011*).

[30] Nigeria National Petroleum Corporation - NNPC. (2010). Annual statistics bulletin. www.nnpcgroup.com . *accessed on 10th March, 2012).*